Structural, morphological and impedance spectroscopic studies on (1-x)$Pb(NO_3)_2$: xCeO_2 composite solid electrolytes

Govind Reddy.Y[1], Sadananda Chary.A[1], Awasti.A.M[2], Narender Reddy.S[3*]

[1]*Department of Physics, University College of Science, Osmania University, Hyderabad 500007, India*
[2]*Thermodynamics Lab, UGC-DAE Consortium, Indore 452017, India*
[3]*Department of Physics, University College of Engineering, Osmania University, Hyderabad 500007, India*

[*]Corresponding author, Tel: (+91)-9949055469; E-mail: snreddy_sattineni2000@yahoo.com

Received: 09 November 2016, Revised: 30 March 2017 and Accepted: 19 April 2017

DOI: 10.5185/amp.2017/985
www.vbripress.com/amp

Abstract

The composite solid electrolyte systems, (1-x)$Pb(NO_3)_2$:xCeO_2 (x= 0, 0.02, 0.03, 0.04, 0.05 and 0.08), have been investigated by XRD for structural properties, SEM with EDS for morphological studies and Electrical properties through impedance spectroscopy. The frequency and temperature dependence of ac conductivity, dielectric constant and dielectric loss were measured between the temperatures 30^{o}C to 340^{o}C in the frequency range 1Hz to 10MHz. The complex impedance data is analyzed in conductivity, permittivity and electric modulus formalism in order to through light on transport mechanism. Variation of ac conductivity against frequency suggests the response obeying universal power law. The dynamics of conducting ion is studied through Jonscher's Universal power law. The parameters of n and A of Jonscher's Universal law suggest these values are strongly temperature sensitive. The variation of dielectric permittivity, loss, and modulus spectra were found to be consistent with conductivity. Impedance, dielectric and modulus analysis had indicated the non-Debye behavior in these composites. The relaxation phenomena were observed in all formalisms. Copyright © 2017 VBRI Press.

Keywords: Composite solid electrolyte, ac conductivity, dielectric relaxation, fluorite type structure, lead nitrate.

Introduction

Inorganic materials are important candidates in the field of solid electrolytes. The ionic conductivity in these materials is sensitive to composition and structure [**1**]. The enhancement of ionic conductivity especially at low temperatures is important for the development of solid state ionic devices, such as batteries, fuel cells, chemical sensors etc [**2**]. Conductivity of certain ionic solids can be significantly enhanced by employing a novel technique called heterogeneous doping with chemically inert, ultrafine and highly insulating particles such as Al_2O_3, CeO_2, SiO_2, ZrO_2, Fe_2O_3 etc. A large number of two phase composite systems have so far been investigated and the conductivity enhancement by one to three orders of magnitude with respect to the conductivity of pure system has been reported. For all composite systems, existence of space charge region between host and dispersoid is attributed for the enhancement of conductivity [**3**-**4**].

Impedance Spectroscopy (IS) is a nondestructive technique to analyze electrical and electrochemical properties of various types of materials. Impedance data from the complex impedance measurements have been analyzed in various formalisms such as impedance (Z*), permittivity (ϵ*) and electric modulus (M*) over a wide range of frequency and temperature to study relaxation properties of material. Electrode polarization which is unavoidable in dielectric and impedance formalisms can be avoid in the analysis of data through electric modulus representation [**5**].

The fluorite structure consists of a simple cubic lattice, cubic corners being occupied by the anions with the centers of the alternative cubes being occupied by cations. In this structure charge transfer takes place through motion of anions [**6**]. The nitrates of Ca, Ba, Sr and Pb are isomorphous members of cubic system with fluorite type structure [**7**]. Lead Nitrate ($Pb(NO_3)_2$) belongs to $Pa\bar{3}$ space group and the structure is built up by cubic face centered type arrangement of Pb^{2+} ions with nitrate groups in between. This inorganic solid lead nitrate is known to be ionic conductor with an anti-Frenkel disorder [**8**] taken as host material for the present study.

Some basic characterization studies on composites of $Pb(NO_3)_2$:CeO_2 have also been reported elsewhere[**9**]. The present investigation on (1-x)$Pb(NO_3)_2$:xCeO_2 composite deals with structural, morphological and impedance spectroscopic studies in different formalism for different mole percentages (mol%) with temperature and frequency to understand the ionic conductivity mechanism with an aim to enhance the ionic conductivity. Cerium Oxide

(CeO_2) is opted as dispersoid in present host, which also has fluorite structure.

Materials and methods

Materials

The starting host material Lead Nitrate ($Pb(NO_3)_2$) obtained from Merck chemicals with stated purity of 99%. High purity ultra fine nano size insulating oxide CeO_2 (Sigma Aldrich<25nm) used as dispersoid material.

Preparation of composites

Single crystals are grown by dissolving $Pb(NO_3)_2$ in double distilled water through slow evaporation method. The crystals so grown were made into fine powder by using an agate mortar. The powder was sieved with No.500 mesh to obtain uniform particle size. For host material, dispersoid in 4, 6,8,10 and 14mol% were mixed thoroughly by mechanical milling in an agate mortar with pestle in the presence of acetone. The process of grinding was continued until the homogeneous dispersion of CeO_2 particles in the composite systems. These prepared powders were made into pellets of 12mm diameter and 1-2mm thickness by using a steel dye with hydraulic press at a pressure of 0.26GPa. These pellets were sintered at 300^{o}C for 15hours. After polishing the surfaces, silver paste was applied for good electrical contact.

Measurement and characterization

The prepared composites characterized with XRD and SEM. X-ray diffraction patterns of the samples in powder form were recorded for a Bragg's angle from 10^o to 80^o by using Expert Pro with Cu-K_α radiation of 1.54A^o wavelength at room temperature to carryout phase analysis. Sintered pellets were used to record SEM [ZEISS EVO 18], EDAX [JEOL JSM 5600] to determine microstructure. The impedance measurements were performed using software controlled 'NOVO Control Alpha-A' impedance analyzer in the broad frequency range 1Hz to 10MHz over a temperature range 30^{o}C to 340^{o}C at UGC-DAE consortium for Scientific Research –India, to study ionic conductivity, dielectric properties and its electric modulus.

Results and discussion

Structural studies are performed with X-Ray Diffraction (XRD) for prepared composites. **Fig.1** shows the XRD patterns of pure host, dispersoid and different mol% of CeO_2 composites. XRD patterns of (1-x)$Pb(NO_3)_2$:xCeO_2 samples clearly show biphasic nature i.e. $Pb(NO_3)_2$ and CeO_2 peaks remain separated and intensities of peaks corresponding to dispersoid proportionately increase with increase in mol% of dispersoid. From XRD data the values of average crystallite size, lattice constant and relative density of composites are calculated and are shown in **Table 1**. An overall reduction in crystallite size can be noticed with dispersion. It can be attributed to mismatch of cationic sizes of host (Pb^{2+}=1.19A^o) and dispersoid (Ce^{4+}=1.02A^o), which leads to increase in lattice strain [**10**]. Densities (ρ) of all composites are estimated by using Archimedes principle. It can be observed that densities of all composites are lower than that of host. Decrease in density indicates uniform distribution of dispersoid in the host leading to formation of space charge regions. The variation of crystallite size and densities clearly signifies enhancement in lattice defects in dispersed composites. The enhancement of defects through dispersion is pivot to enhance ionic conductivity and dielectric constant for any composite system [**3**].

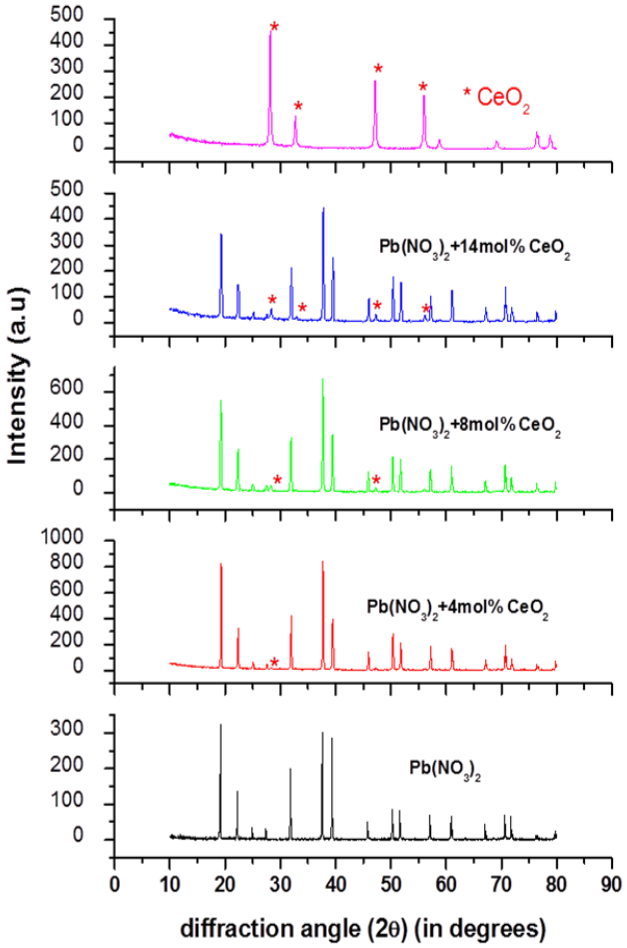

Fig. 1. XRD patterns of host, dispersoid and composites at different mol%.

Table 1. XRD data for $Pb(NO_3)_2$ dispersed with different mol% of CeO_2.

mol% of composite	Crystallite size (nm)	Lattice constant (A^o)	Relative Density (%)
0	149.23	8.0327	93.73
4	37.11	7.9112	88.35
6	37.11	7.9072	90.46
8	55.76	7.9151	88.67
10	37.01	7.9358	86.31
14	55.64	7.9013	86.33

SEM analysis on different composites provides information about surface morphology, distribution of dispersoid particles in the composite system. **Fig. 2** (**a to d**) shows the SEM images with corresponding EDS of pure lead nitrate and different (4, 8 and14mol %) dispersed composites. SEM image of pure lead nitrate **(Fig.2a)** shows different sized grains distributed throughout the sample. The unequal sizes of grains may be due to sintering effect. A change in surface morphology can be seen clearly between host and dispersed composites. SEM micrographs support calculated data from XRD results shown in **Table 1**, in terms of reduced crystallite size and decrease in relative density between host and dispersed composites. In two phase composite systems grain size of host may decrease and display low dense surface with enhanced defects [**11**]. The interface interaction between host and dispersoid are accountable for the creation of these defects. Formation of a new region called space charge region between them causes the modifications in the properties such as electrical transport and thermal properties [**12**]. Out of 4, 8 and 14mol% dispersed composites a favorable microstructure is observed for 8mol%, in terms of reduced crystallite size, which in terms induce optimum crystal defects, there by optimum enhancement in conductivity in this system.

EDS pictures of pure and different composite systems are shown in **Fig.2** along with the corresponding SEM micrographs. They reveal the biphasic nature of composite systems. EDS studies show the presence of all elements (Nitrogen, Oxygen, Ceria and Lead) corresponding to host and dispersoid in their proportionate quantities. This indicates parent compounds are undisturbed or unmodified after sintering.

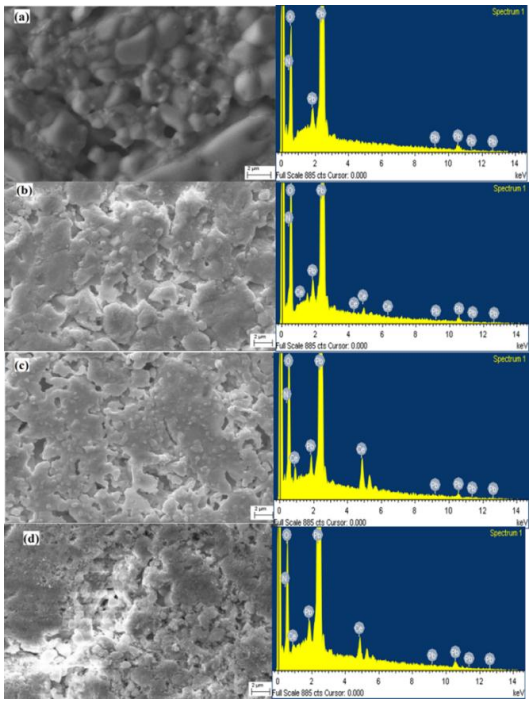

Fig. 2. SEM images and its EDS pictures of (a) pure $Pb(NO_3)_2$ (b) $Pb(NO_3)_2$ + 4mol% of CeO_2 (c) $Pb(NO_3)_2$ + 8mol% CeO_2 (d) $Pb(NO_3)_2$+14mol% of CeO_2.

At ideal conditions Nyquist plot consists of three semicircles corresponding to grain contribution at higher frequencies, grain boundary contribution at moderate frequencies and electrode/electrolyte interface at low frequencies, starting from origin [**13**]. Nyquist plots are drawn at different temperatures for 8mol% dispersed CeO_2 composite for which maximum enhancement of conductivity was observed as shown in **Fig. 3**. Inset graphs show Nyquist plots at higher temperatures (90°C, 160°C). The shape of Nyquist plots at lower temperatures consists of two distinct regions. Starting from origin first depressed semicircle corresponds to bulk and grain boundary contribution and a spike appears at very low frequency corresponds to electrode polarization. It can be observed that with increase in temperature (inset graph at 90°C) spike like line disappears and the first depressed semicircle resolves into two separate semicircles corresponding to bulk of the sample and grain boundary respectively. With further increase in temperature, first of these two depressed semicircles appears to decrease slowly in its diameter implying lesser contribution from the bulk to the total conductivity where as the second depressed semicircle expands resulting increase in grain boundary contribution to the total conductivity. As can be seen from the inset at 160°C, the semicircle pertaining to bulk becomes parallel line to imaginary axis indicating its capacitive nature, where as the second depressed semicircle corresponding to grain boundary is wholly responsible for the conductivity at this and other higher temperatures. Grain boundary contributions for ionic conductivity in other composite systems reported in literature are in agreement with observation [**14-16**]. Similar Nyquist plots were also observed for 4 and 6 mol% dispersed composites. Morphological studies of dispersed systems with SEM clearly indicate change in surface morphology of composites in terms of more clustering nature of grains with more empty space. Increase in empty space is associated with easier mobility of charge carriers, thereby increase in conductivity [**17**].

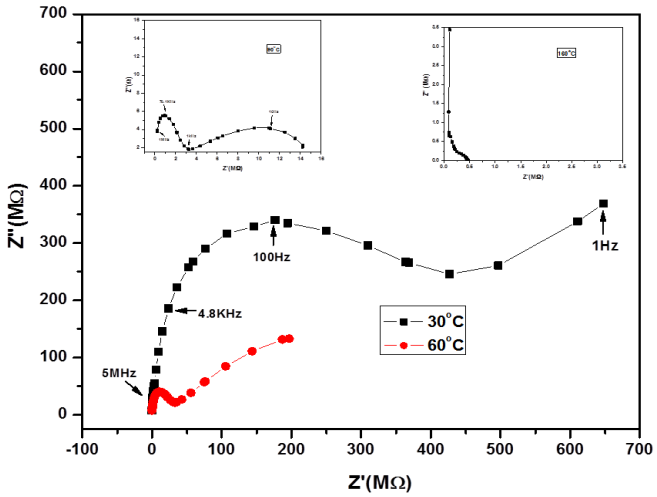

Fig. 3. Nyquist plots for 8mol% dispersed composite at different temperatures. Two inset graphs are Nyquist plots at 90°C and 160°C for 8mol% dispersed composite.

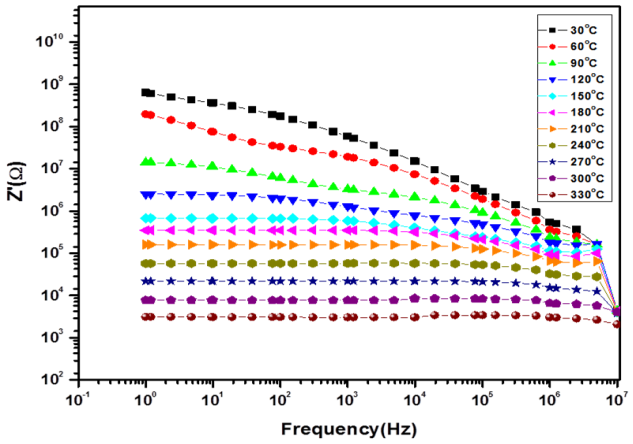

Fig. 4. Variation of Z′ with frequency for 8mol% dispersed composite, temperature as parameter.

To understand impedance properties in different formalism we also studied, frequency Vs real part of impedance and imaginary part of impedance. **Fig. 4** shows variation of real part of impedance (Z′) with frequency for 8mol% of CeO_2 dispersed composite throughout temperature range. The decrease of Z′ constantly with temperature and frequency indicates increase in conductivity. The response of Z′ with temperature indicates existence of temperature dependent electrical relaxation for the present composite. The existence of relaxation for the present system can be studied from imaginary part (Z") of impedance with frequency. **Fig. 5** shows variation of Z" with frequency for 8mol% dispersed CeO_2 throughout the temperature range. It is observed that Z" continuously decreases linearly with temperature. Existence of relaxation peaks can be observed throughout the temperature range. With increase in temperature, size of second relaxation increases continuously, whereas the contribution of first relaxation peak continuously decreases and finally disappears. This feature is clearly shown in the inset graph drawn between frequency Vs Z" from 30°C to 150°C temperature. These results are in accordance with analysis of Nyquist plots for impedance. The peak broadening indicates deviation from ideal Debye nature for this composite. The shape of relaxation peaks indicates non Debye type relaxation [**18**].

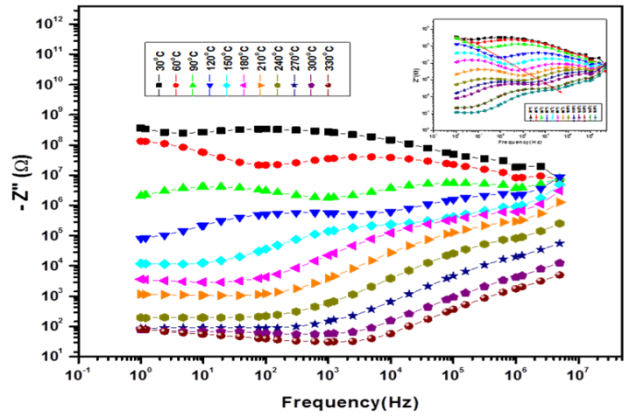

Fig. 5. Variation of Z" with frequency at different temperatures for 8mol% dispersed composite. Inset graph shows frequency Vs Z" between room temperature to 150°C.

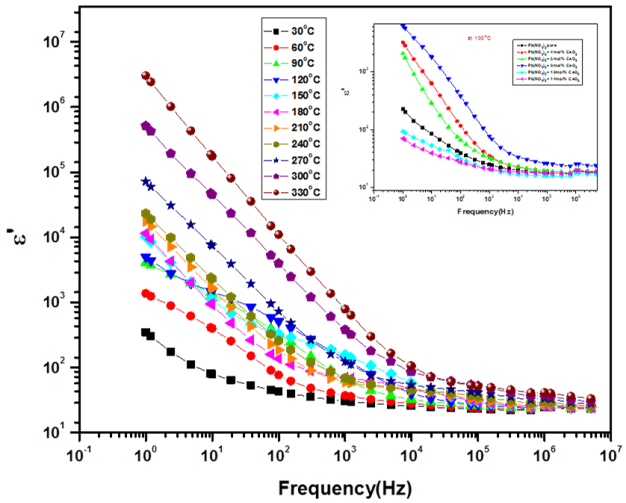

Fig. 6. Variation of dielectric constant (ε′) with frequency for 8mol% dispersed composite between 30°C to 330°C. Variation of ε′ with frequency for all composites at 100°C is shown as inset.

The analysis of data with dielectric formalism provides insight into ionic transport phenomena and response of different polarizations with frequency and temperature. **Fig. 6** shows logarithmic variation of dielectric constant (ε′) with frequency, temperature as parameter for 8mol% dispersed composite. Inset graph shows variation of ε′ with frequency for various dispersed composites at 100°C. Dispersion of ε′ can be seen at low frequency region and becomes saturated at high frequencies [**19**]. With increase in frequency the ionic and orientational polarizabilities decrease and finally disappear leading to a constant value (ε_∞) of dielectric permittivity. The magnitude of ε′ in the low frequency region can be seen to increase with temperature. The dispersion at low frequency region can be attributed to the accumulation of space charge within the electrolyte conforming non-Debye nature of relaxation. Such observations were reported in other ion conducting dielectrics where motion of ions is associated with ion hopping mechanism [**20**].

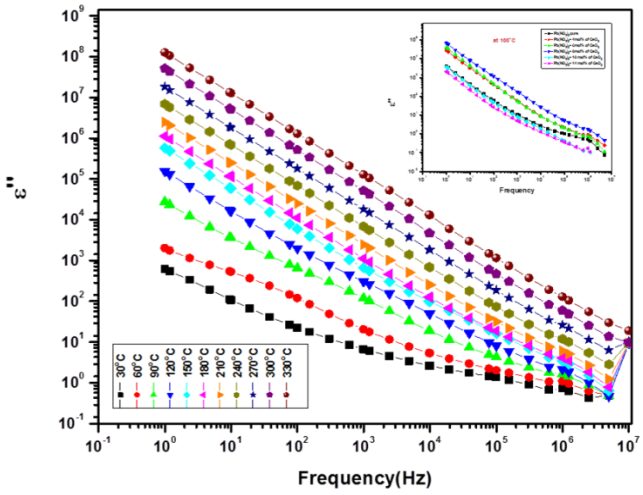

Fig. 7. Variation of dielectric loss with frequency at different temperatures for 8mol% composites. Inset figure shows ε" Vs frequency for different composites at 100°C.

Fig. 7 shows variation of ε" (dielectric loss) with frequency for 8mol% dispersed composite at different temperatures. Inset graph shows ε" Vs frequency for different dispersed composites at a typical temperature of 100°C. It is observed that dielectric loss decreases linearly with frequency and temperature throughout experimental range, without any loss peak. The absence of dielectric loss peak in electrolytic materials in general is due to unavoidable electrode polarization [**18**]. Loss due to motion of ions and that associated with ionic polarization can be considered as responsible factors for dielectric loss at low and moderate frequencies, whereas at high frequencies it could be due to ionic vibrations. Response of both the dielectric parameters (ε′ and ε") have shown increasing trend with temperature which can be attributed to enhanced charge carrier density arising out of ion dissociation aggregates.

Loss tangent is the ratio of dielectric loss (ε″) to dielectric constant (ε′) i.e. $Tan\ \delta = \frac{\varepsilon''}{\varepsilon'} = \frac{M''}{M'} = \frac{Z'}{Z''}$. The measurement of loss tangent can provide information about dielectric relaxation in ionic conductors. **Fig. 8** shows the variation of loss tangent (tanδ) on log scale with frequency for 8mol% dispersed composite at typical temperatures, inset graph shows variation of tanδ with frequency at 100°C for all the composites. The loss tangent peak observed is seen to shift to high frequency with increase in temperature. Existence of tanδ peak at low frequencies denotes conductivity dominated by DC. Each individual peak initially observed to increase with frequency and attains maximum at a particular frequency. This can be attributed to thermally activated relaxation process for ion conducting composites [**21**]. Studies on electric modulus analysis provide information about ion dynamics and mechanism of conductivity relaxation as a function of frequency and temperature, related to bulk properties of samples by suppressing electrode effect which is unavoidable in impedance and dielectric formalism. Variation of real part of modulus (M′) with frequency for 8mol% dispersed composite at different temperatures is shown in **Fig. 9**. The values of M′ are found to negligible at lower frequencies and increases at higher frequencies for all temperatures in the form of sigmoid. The values of M′ starting from negligible at low frequencies indicate the absence of electrode effect. It is found that M′ reaches to a constant value at higher frequencies and is attributed to conduction phenomena due to short range mobility of charge carriers [**22**]. The sigmoid shape of variation can be seen to shift higher frequencies as temperature increases. This behavior supports the long range mobility of charge carriers [**22**].

Fig. 10 shows variation of M″ with frequency at various temperatures for 8 mol% dispersed composite system. The curves are asymmetrically resolved over a range of frequency which is an indication of dispersive nature of composite system with one maximum relaxation peak at a frequency (f_m). Frequency range below f_m indicates that charge carriers are mobile over a long distance i.e. ions can take successive hopping from one site to other. Frequency range above f_m corresponds to the charge carriers confining to short distances [**22**]. The peak occurring region indicates transition of mobile ions from long range to short range motions. The peak frequency f_m is found to increase with temperature leading to a decrease in relaxation time, which suggests that the relaxation is a thermally activated phenomenon and existence of charge carrier hopping [**23**]. The relaxation time ($\tau_p=1/2\pi f_m$) is found to decrease with temperature, which in turn results in increase in conductivity. Inset figure shows a linear relationship between relaxation time τ_p and inverse of absolute temperature and can be described as Arrhenius relation $\tau_p = \tau_o e(-E_a/KT)$ where the symbols have their usual meaning. The value of activation energy is estimated as 0.58eV between temperature 80 and 280°C. Shifting of peak frequency towards higher frequencies also indicates that there is an increase in ionic conduction [**24**].

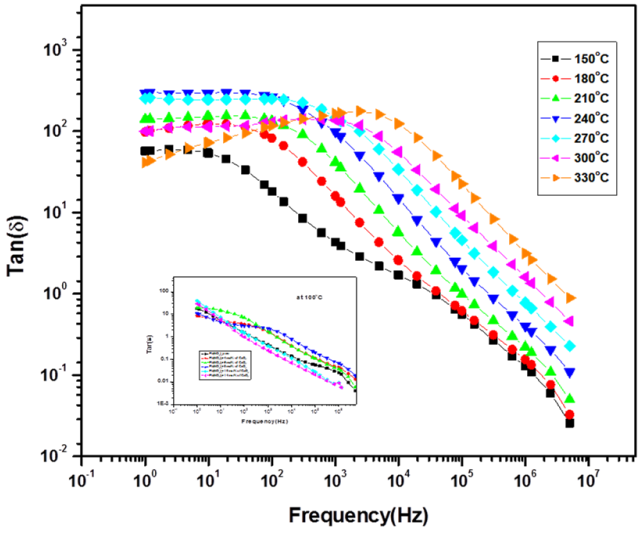

Fig. 8. Variation of loss tangent (tanδ) with frequency for 8mol% composite and inset graph is for different composites at 100°C.

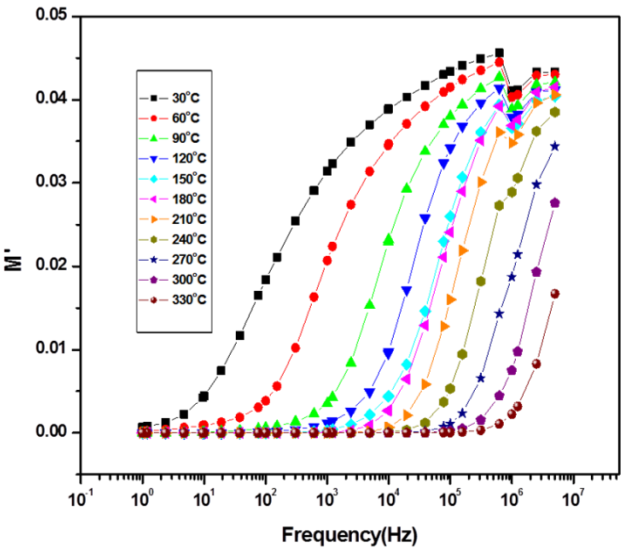

Fig. 9. Variation of real part of electric modulus (M′) with frequency for 8mol% composite.

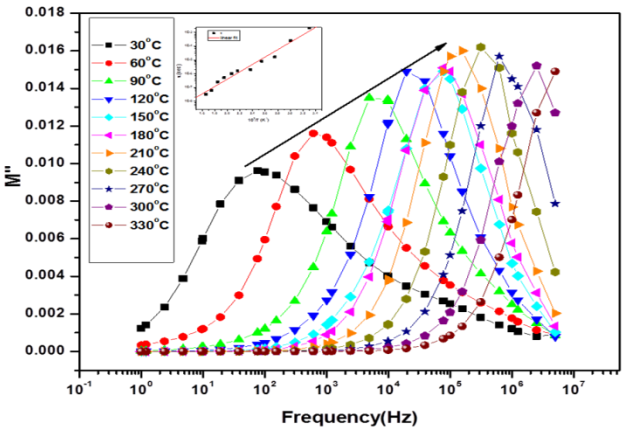

Fig. 10 Variation of imaginary part of Modulus (M") with frequency at temperature range 30°C to 330°C for 8mol% dispersed composite. Inset graph is inverse of absolute temperature Vs relaxation time.

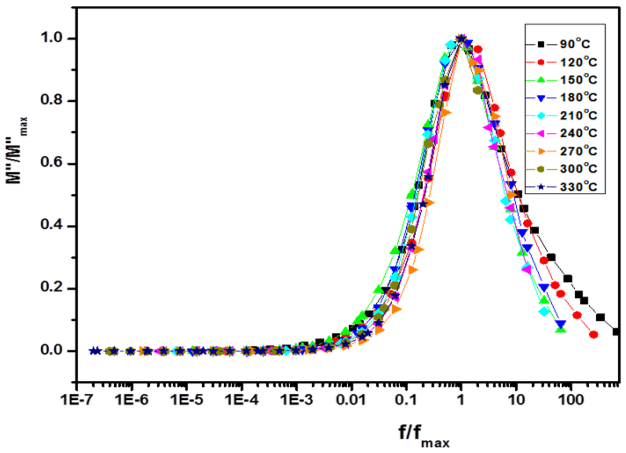

Fig. 11. Scaling studies for 8mol% composite between 90°C to 330°C.

The scaling studies of the modulus spectra provide an insight into the composition and temperature dependent of the relaxation dynamics [**25**]. **Fig. 11** shows normalized plots (M''/M''_{max} Vs f/f_{max}) at different temperatures of 8mol% dispersed system. The near overlap of these curves into a single master curve suggests that all relaxation mechanisms occurring at different frequencies are temperature independent. Variation of Z″ and M″ parameters with frequency at a typical temperature of 100°C is shown in **Fig. 12**. The relaxation peak pertaining to Z″ arises at lower frequency where as M″ relaxation peak at a high frequency indicating the existence of non-Debye type of relaxation [26, 5]. Variation of ac conductivity with frequency at typical temperatures for 8mol% composite on log-log scale is shown in **Fig. 13**. The frequency dependent conductivity is found to follow Jonscher's universal power law [**27**]. According to it $\sigma_{ac}(\omega) = \sigma(o)+A\omega^n$, where σ(o) is dc conductivity, A is dispersion parameter and n is dimensionless frequency exponent whose value lies in the range 0 to 1. Its second term $A\omega^n$ corresponds to frequency dependent ac conductivity. The value of n represents the degree of interaction between the mobile ions to the lattice around them and A determines the strength of polarizablity. If n is equal to zero random hopping (frequency independent of conductivity) of carriers takes place and if it is tending to 1 denotes increase in correlation. The values of σ_0, A and n are extracted by standard fitting to ac conductivity data. The fitted values are shown in **Table 2** for selected range of temperature. The value of n is found to vary from 0.11 to 0.96 in the temperature range 30°C to 330°C, suggesting that the fitted value of 'n' is within the theoretical limit. The variation of n and A parameters with temperature is shown in the inset of **Fig. 13**, which indicates they are temperature dependent. The value of n is found to increase, while there is decrease in the value of A with temperature. The variation of n value strongly suggests that there exist more than one hopping mechanism.

Table 2. The values of σ_o, A and n at different temperatures for 8mol% CeO_2 dispersed composite solid electrolyte.

Temperature (°C)	σ_0(S/cm)	A ($Scm^{-1}rad^{-n}$)	n
180	$6.4945x10^{-7}$	$1.7x10^{-4}$	0.5672
190	$9.2112x10^{-7}$	$1.1x10^{-4}$	0.5927
200	$1.1338x10^{-6}$	$4.0x10^{-5}$	0.6461
210	$1.4415x10^{-6}$	$2.9x10^{-6}$	0.8091
220	$2.0074x10^{-6}$	$3.7x10^{-7}$	0.9345
230	$2.8308x10^{-6}$	$1.9x10^{-7}$	0.9673
240	$3.9066x10^{-6}$	$1.8x10^{-7}$	0.9651
250	$5.2083x10^{-6}$	$1.6x10^{-7}$	0.9632
260	$7.6373x10^{-6}$	$1.5x10^{-7}$	0.959
270	$1.0151x10^{-5}$	$1.7x10^{-7}$	0.9456
280	$1.3461x10^{-5}$	$3.2x10^{-7}$	0.8941

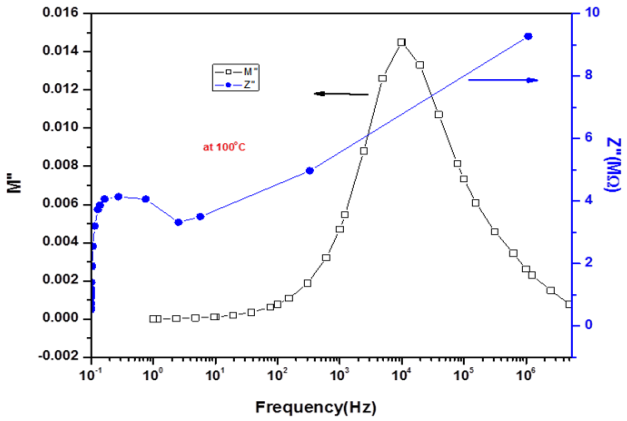

Fig. 12. Z", M" Vs frequency at 100°C temperature for 8mol% composite.

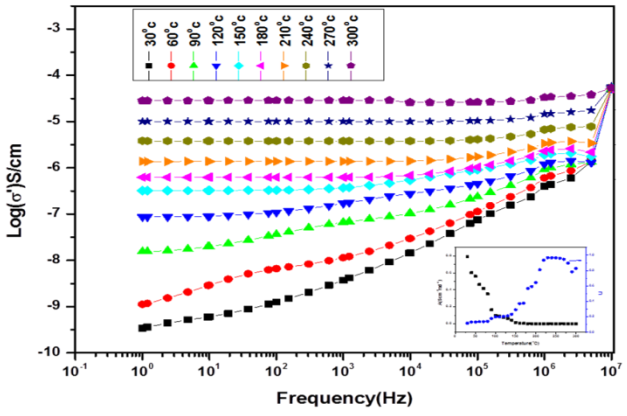

Fig. 13. Variation of ac conductivity on log-log scale for 8mol% composite between 30°C and 330°C and inset is the response of n and A from fitted data.

According to Jump Relaxation Mechanism (JRM) model proposed by Funke and co workers to study ion dynamics in disordered solids, ion conduction takes place through local hopping motions at lower frequencies and through vibrations in IR range [**28**]. The dc conductivity variation for the present system at low frequencies could be due to hopping of ions from one site to the neighboring vacant site, whereas correlated forward back ward hopping mechanism seems to operate at high frequencies. The frequency dependent conductivity for the present system is well fitted into Jonscher's Universal power law.

The variation of ac conductivity (σ_{ac}) with frequency for all composites with respect to host is shown in **Fig. 14**. The enhancement of conductivity is observed throughout the experimental range of frequency for 4, 6 and 8 mol% CeO_2 dispersed composite systems. Whereas for 10 and 14mol% dispersed composites conductivity enhancement shown a decrement. The enhancement of conductivity is found to increase with mol% up to a threshold 8, after which the fall of enhancement with mol% which could be interpreted as due to blocking effect. Existence of blocking effect is a common phenomenon in all inorganic dispersed solid electrolyte systems [**29**].

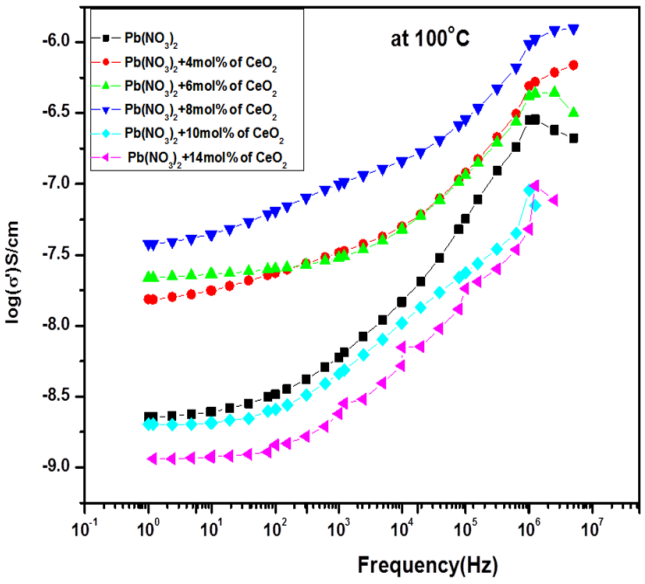

Fig. 14. Variation of ac conductivity with frequency for different composites at 100°C.

Dc conductivity of the present system has been extracted from ac conductivity data (~1Hz). **Fig. 15** shows variation of dc conductivity with temperature for different mol percentages of CeO_2. From figure it can be observed that the enhancement of conductivity with mol% increases up to 8 mol% of dispersoid and a decrement in conductivity was noticed with further increase in mol% of dispersoid. The shape of Arrhenius plots appears like sigmoid shape instead of straight line. According to Voronin et al. it is a common feature in fluorite type structured composite solids [**30**].

Table 3. Ion transport parameters extracted from Arrhenius plots for different mol% of composites Pb(NO3)2:CeO_2 between temperature range 80-280°C.

mol% of composite	Activation Energy (E_a)eV	Pre exponential factor (σ_0)
0	0.75	1.6107
4	0.62	0.2621
6	0.59	0.3862
8	0.58	0.0131
10	0.79	2.0352
14	0.85	2.4426

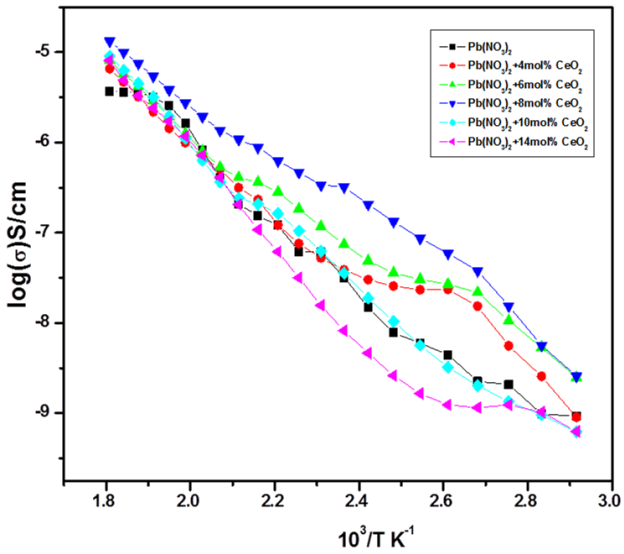

Fig. 15. Arrhenius plots for different mol% of composites and host.

Activation energies are calculated for all composites and are shown in **Table 3**. It is observed that up to 8mol% dispersion activation energy (E_a) is found to decrease and then increased there after i.e. least activation energy recorded for highest conducting composite. The increase in concentration of point defects in the space charge region formed between the host and dispersoid is supposed to be responsible for the enhancement of conductivity in these systems. The enhancement of conductivity for the present composites can be understood from Maier's space charge model [**31**]. $Pb(NO_3)_2$ being an anti-Frenkel defect solid, NO_3^- ions are either attracted or repelled to the surface of the dispersed due to the chemical affinity. This leads to increase in vacancy concentration there by formation of space charge region at interface. It is presumed that for present composite system formation of NO_3^- ion vacancy more probable. Conduction of NO_3^- ion in solid membrane is reported in literature [**32**]. Apart from this influence of mechanical strain for enhancement of conductivity of composites cannot be ruled out. Because mismatch in ionic sizes of host and dispersoid leads to increase in strain at interface of host and dispersoid [**3**].

Conclusion

The present composite (1-x)$Pb(NO_3)_2$:xCeO_2 system shows maximum conductivity for 8mol% dispersion of CeO_2 with respect to host. Impedance studies reveal that grain boundary contribution increases with temperature. The phenomenon of relaxation is studied through impedance, dielectric and electric modulus formalism. Shifting of peak frequency of loss tangent (tanδ) from low frequency to high frequency indicates thermally activated relaxations for the present composites. For enhancement of ionic conductivity, the enrichment of interstitials which leads to formation of space charge region between the host and dispersoid is supposed to be responsible. Activation energies (E_a) extracted from dc conductivity studies has shown least value for 8mol% composite. Frequency dependent conductivity obeys Jonscher's Universal power law for all composites. The XRD and SEM studies conform biphasic nature of composites. EDS studies confirm presence of all parent elements in composites at their proportionate value.

Acknowledgements

Authors would like to acknowledge the Head, Department of Physics, Osmania University and director UGC-DAE (Indore) for allowing to use experimental facilities.

Author's Contributions

Conceived the plan: ASC, SNR; Performed the experiments: YGR; Data analysis: SNR, ASC, AMA; Wrote the paper: YGR, SNR, ASC. Authors have no competing financial interests.

References

1. Wang, Yu.; Zhong, Wei-Hong; *ChemElectroChem*, **2015**, *2*, 22.
2. Tadanaga, Kiyoharu.; Imai, Katsuya.; Tatsumisago, Masahiro.; Minami, Tsutomu; *J. of the Electrochem. Soc.*,**2002**, *149* (6), A773.
3. Uvarov, N.F; *J. Solid State Electrochem*, **2011**, *15*,367.
4. Gupta, Archana.; Sil, Anjan.; Verma, N.K; *J. of physics and chemistry of solids*, **2009**, *70*,340.
5. Patro, L.N.; Hariharan, K; *Ionics*, **2013**, *19*, 643.
6. V.Kharton, Vladislav.; Solid State Electrochemistry 1: Fundamentals, Materials and their Applications; Wiley-VCH : Germany, **2005**.
7. Sai babu, K.; Chiranjivi, T; *Solid State Ionics*, **1984**,*13*,7.
8. Saibabu, K; Chiranjivi, T; *Solid State Ionics*, **1983**, *11*, 45.
9. Govind Reddy, Y.; Sadananda Chary, A.; Narender Reddy,S; *Materials Science Research India*, **2015**, *12*(2), 89.
10. Kour, P.; Kumar, Pawan.; Sinha, S.K.; Kar, Manoranjan; *Solid State communications*, **2014**, *190*, 33.
11. Desvals, M.A.; Knauth, P; *j.phys.chem.solids*, **1997**, *58*(2), 319.
12. Zafar Iqbal, Mohd.; Rafiuddin; *Measurement*, **2016**, *18*,102.
13. Barsoukev, Evgenij.; Macdonald, J.Ross.; Impedance Spectroscopy Theory, Experiments and Applications; John Wiley: USA, **2005**.
14. Chung, Habin.; Kang, Byoungwoo; *Solid State Ionics*, **2014**, *263*, 125.
15. Cho, Pyeong-Seok.; Park, Seung-Young.; Kim, Jeong-Joo.; Do, Hyoung-Seok; Park Jong-Heun Lee, Hyun-Min; *Solid State Ionics*, **2010**, *181*, 1420.
16. Brahma, Sanjaya.; Choudhary, R.N.P.; Shivashankar S.A; *J. of Phy. and Chem. of Solids*, **2012**, *73*, 357.
17. Nath, A.K.; Kumar, A; *Electrochem. Acta*, **2014**, *129*, 177.
18. Anantha, P.S.; Hariharan, K; *Materials Science and Engineering B*, **2005**, *121*, 12.
19. Saidi, K.; Kamoun, S.; Ferid Ayedi, H.; Arous, M; *J. of phy. and chem.. of solids*, **2013**, *74*, 1560.
20. Mariappan, C.R.; Govindaraj, G; *Materials Science and Engineering B*, **2002**, *94*, 82.
21. Wang, Chunchang.; Zhang, Nan.; Li, Qiuju.; Yu, Yi; Zhang, Jian.; Li, Yide.; Wang, Hong; *J.Ame.Ceram. Soc*., **2015**, *98*(1), 148.
22. Mishra, Amodini.; Choudhary, S.N.; Prasad, K.; Choudhary, R.N.P; *PhysicaB*, **2011**, *406*, 3279.
23. Wang, Jing.; Li, Qiuju.; Yu, Yi.; Zhang, Jian.; Zheng, Jun.; Chenng, Chao.; Li, Yide.; Wang, Hong.; Wang, Chuchang; *PhysicaB*, **2014**, *447*, 62.
24. Tiwari, Tuhina.; Kumar, Manindra; Srivastava, Neelam.; Srivastava, P.C; *Material Science and Engineering B*, **2014**, *182*, 6.
25. Karmakar, A.; Ghosh, A; *Current Applied Physics*, **2012**, *12*,539.
26. Padmasree, K.P.; Kanchan, D.K.; Kulkarni A.R; *Solid State Ionics*, **2006**, *177*, 475.
27. Jonscher, A.K; Dielectric relaxation in solids; Chelsea Dielectric press: London, **1983**.
28. Funke, K; *Solid State Ionics*, **1997**, *94*, 27.
29. Anantha, P.S.; Hariharan, K; *J.Phys.Chem. Solids*, **2003**, *64*, 1131.
30. Voronin, B.M.; Volkov, S.V; *J. of Phy. and Chem. of Solids*, **2001**, *62*, 1349.
31. Maier, J; *Prog.Solid St. chem.*, **1995**, *23*,171.
32. Maria, J.Ariza.; Toribio, F.Otero; *Journal of Membrane Science*, **2007**, *290*, 241.

